Solving the Nernst-Planck Equation in Heterogeneous Porous Media with Finite Volume Methods: Averaging Approaches at Interfaces

Christophe Tournassat[1,2,3*], Carl I. Steefel[1], and Thomas Gimmi[4,5]

[1]Lawrence Berkeley National Laboratory, 1 Cyclotron Road, Berkeley, CA 94720, USA.

[2]BRGM, 3 avenue Claude Guillemin, 45060 Orléans, France.

[3]Université d'Orléans – CNRS/INSU – BRGM, UMR 7327 Institut des Sciences de la Terre d'Orléans, 45071 Orléans, France.

[4]Rock-Water Interaction, Institute of Geological Sciences, University of Bern, CH-3012 Bern, Switzerland.

[5]Laboratory for Waste Management, Nuclear Energy and Safety, Paul Scherrer Institut, CH-5132 Villigen, Switzerland.

Corresponding author: Christophe Tournassat (ctournassat@lbl.gov)

Key Points:

- Solving the Nernst-Plank equation with a finite volume method requires a proper averaging procedure of properties at grid cell interfaces.
- Averaging rules commonly applied to diffusion properties can lead to numerical instability and result in inaccuracy in reactive transport codes.
- Correct averaging schemes were derived for the general case.

Abstract

Molecular diffusion of dissolved species is a fundamental mass transport process affecting many environmental and technical processes. Whereas diffusive transport of single tracers can be described by Fick's law, a multicomponent approach based on the Nernst-Planck equation is required for charge-coupled transport of ions. The numerical solution of the Nernst-Planck equation requires special attention with regard to properties that are required at interfaces of numerical cells when using a finite difference or finite volume method. Weighted arithmetic and harmonic averages are used in most codes that can solve the Nernst-Planck equation. This way of averaging is correct for diffusion coefficients, but inappropriate for solute concentrations at interfaces. This averaging approach leads to charge balance problems and thus to numerical instabilities near interfaces separating grid volumes with contrasting properties. We argue that a logarithmic-differential average should be used. Here this result is generalized, and it is demonstrated that it generally leads to improved numerical stability and accuracy of concentrations computed near material interfaces. It is particularly relevant when modeling semi-permeable clay membranes or membranes used in water treatment processes.

1 Introduction

Diffusion of aqueous species in geological or engineered media is a fundamental mass transport process. It is especially important for low permeability geological materials containing significant amount of clay minerals such as clayey shales, engineered materials such as clay barriers, or concrete structures. Their low permeability and diffusion properties make them ideal for waste confinement applications, or technological materials such as filtration membranes used for water treatment. The characterization of diffusion processes is also essential for our ability to understand various hydro-geochemical observations such as isotopic fractionation coupled to transport processes (La Bolle & Fogg, 2001; Peeters et al., 2002; Bourg & Sposito, 2007; La Bolle et al., 2008; Bourg et al., 2010; Rolle et al., 2010), the dynamics of gas-water exchanges (Haghighi et al., 2013; Tokunaga et al., 2017), or the dynamics of contaminant accumulation and release in and from rocks and sediments having very heterogeneous pore structures (Chapman & Parker, 2005; Liu et al., 2006, 2011; Gouze et al., 2008; Robinet et al., 2012; Hadley & Newell, 2014; Zachara et al., 2016; Bone et al., 2017). Ultimately, diffusion is the fundamental process that generates mixing of dissolved species, and enables reactive fronts to appear between aqueous solutions having contrasted chemical compositions (Anna et al., 2011, 2013; Le Borgne et al., 2011, 2013).

Diffusion processes are the result of random motion of dissolved species subject to thermal agitation, and for which no interactions between the dissolved species are considered. Diffusion processes are commonly simulated with Fick's laws. However, ions are charged species, and their individual diffusion coefficients in solution are dependent on their charge, mass and radius. As a consequence of the electro-neutrality condition in aqueous environments, ions are affected by electrochemical migration effects, and multicomponent diffusion processes are thus better represented by the more general Nernst-Planck formulation rather than by the limiting Fick's laws. The importance of electrostatic interactions among charged species in the modeling of multicomponent diffusion processes was early emphasized to explain vertical profiles of ion concentrations in the pore water of marine sediments, i.e. systems in which diffusion is the dominant transport process (Ben-Yaakov, 1972; Lasaga, 1979; Felmy & Weare, 1991a; b; Giambalvo et al., 2002; Boudreau et al., 2004). Later the importance of multicomponent

diffusion in our understanding of mixing processes in porous media has been demonstrated even for systems whose mass transport is dominated by advective flow (Chiogna et al., 2011; Muniruzzaman et al., 2014; Muniruzzaman & Rolle, 2015, 2016, 2017; Rasouli et al., 2015; Rolle et al., 2018). In the field of reactive transport modeling, the use of multicomponent diffusion models is hindered by two factors: the first one is the scarcity of codes that are able to handle the Nernst-Planck formulation for the resolution of diffusive fluxes (Steefel et al., 2015); the second one is the computational cost associated with the use of the Nernst-Planck formulation rather than Fick's laws. In the last decade, the use of Nernst-Planck equation instead of Fick's laws has been shown to be essential to understand the apparent anomalous diffusion behavior of systems in which the diffusion of charged species is affected by the electrostatic properties of the surfaces present on the solid phases (Tournassat & Steefel, 2015). Most of the related studies concerned the properties of clay and concrete materials, which are investigated with regard to their confinement properties for radionuclides or other toxic solutes (Gvirtzman & Gorelick, 1991; Appelo & Wersin, 2007; Appelo et al., 2008, 2010; Glaus et al., 2013, 2015; Alt-Epping et al., 2015, 2018; Tournassat & Steefel, 2015, 2019a; b; Bourg & Tournassat, 2015; Tinnacher et al., 2016; Appelo, 2017; Gimmi & Alt-Epping, 2018). However, the use of reactive transport models using the Nernst-Planck formulation can be foreseen to be increasingly important for the modeling of other types of materials and related applications including microbial electrochemical cells or membrane filtration technologies (Marcus et al., 2010).

The numerical solution of the Nernst-Planck equation in a reactive transport model using a finite difference/volume method is subject to a range of difficulties when applied to spatially heterogeneous media (Tournassat & Steefel, 2015; Gimmi & Alt-Epping, 2018). In this study, we address the problem of the definition of averaged properties at the interface between porous domains having contrasting properties. This work should facilitate a rigorous implementation of the Nernst-Planck equation in reactive transport codes.

2 Governing equations

In absence of an external electric potential, the electrochemical potential μ_i (in J·mol^{-1}) of an ion i can be expressed as

$$\mu_i = \mu_i^{\circ} + RT\ln a_i + z_i F\psi = \mu_i^{\circ} + RT\ln\frac{\gamma_i m_i}{m^{\circ}} + z_i F\psi \quad (1)$$

where T is the temperature (in K), R is the gas constant (8.314 J·K^{-1}·mol^{-1}), F is the Faraday constant (96 485 J·V^{-1}·mol^{-1}), ψ an (internal) electrical potential (V), m° is the standard state molality (1 mol·kg^{-1}), μ_i° is the standard (electro)chemical potential of species i (in J·mol^{-1}), a_i is its chemical activity, z_i is its charge number (dimensionless), m_i is its molality (in mol·kg^{-1}) and γ_i is its activity coefficient (dimensionless). The diffusive flux $J_{i,s}$ (in mol·m^{-2}·s^{-1}) of an ion in a solution is given by the Nernst-Planck equation:

$$J_{i,s} = -u_i c_i \nabla\mu_i = -u_i c_i RT\nabla\ln\left(\gamma_i\frac{m_i}{m^{\circ}}\right) - u_i z_i F c_i \nabla\psi \quad (2)$$

where u_i is the mobility of species i (in mol·m^2· s^{-1}·J^{-1}), and c_i is its molarity (in mol·m^{-3}), which can be expanded as:

$$c_i = m_i \rho_{solv} \tag{3}$$

where ρ_{solv} is the density of the solvent (in $kg_{solvent} \cdot m^{-3}_{solution}$). The mobility u_i refers here to the average velocity of a species in solution acted upon by a unit force, independent of the origin of the force (Steefel & Maher, 2009). The diffusion coefficient D_i (in $m^2 \cdot s^{-1}$) of the species *i* is proportional to its mobility according to the Nernst-Einstein equation:

$$D_i = RTu_i \tag{4}$$

In a porous medium, the diffusion coefficient of the species *i* is usually described as a function of the porosity ϕ, of the tortuosity factor τ_i of the medium, which can be specific to each species, and of the self-diffusion coefficient of the species in solution $D_{i,s}$ (Shackelford, 1991):

$$D_{i,e} = \phi \tau_i D_{i,s} \tag{5}$$

The diffusive flux in a porous medium, $J_{i,p}$, can thus be written:

$$J_{i,p} = -D_{i,e}\rho_{solv} m_i \nabla \ln\left(m_i \gamma_i\right) - \frac{z_i F D_{i,e} \rho_{solv} m_i}{RT} \nabla \psi \tag{6}$$

In one dimension, for the sake of simplicity, Eq. (6) becomes:

$$J^x_{i,p} = -D_{i,e}\rho_{solv} m_i \frac{\partial \ln\left(m_i \gamma_i\right)}{\partial x} - \frac{z_i F D_{i,e} \rho_{solv} m_i}{RT} \frac{\partial \psi}{\partial x} \tag{7}$$

As an additional simplifying condition, the value of the solvent density is often considered constant and equal to 1000 $kg_{solvent} \cdot m^{-3}_{solution}$. It follows:

$$J^x_{i,p} = -D_{i,e} c_i \frac{\partial \ln\left(c_i \gamma_i\right)}{\partial x} - \frac{z_i F D_{i,e} c_i}{RT} \frac{\partial \psi}{\partial x} \tag{8}$$

In the absence of an external electric field, there is no electrical current and so:

$$\sum_j z_j J^x_{j,p} = 0 \tag{9}$$

The combination of equations (7) and (9) provides an expression for the gradient of the diffusion potential:

$$\frac{\partial \psi}{\partial x} = -\frac{RT}{F} \frac{\sum_j z_j D_{j,e} c_j \frac{\partial \ln\left(c_j \gamma_j\right)}{\partial x}}{\sum_j z_j^2 D_{j,e} c_j} \tag{10}$$

Consequently, it is possible to express the Nernst-Planck equation with known parameters only, *i.e.*, concentrations, diffusion coefficients, and activity coefficients:

$$J^x_{i,p} = -D_{i,e} c_i \frac{\partial \ln\left(c_i \gamma_i\right)}{\partial x} + z_i D_{i,e} c_i \frac{\sum_j z_j D_{j,e} c_j \frac{\partial \ln\left(c_j \gamma_j\right)}{\partial x}}{\sum_j z_j^2 D_{j,e} c_j} \tag{11}$$

The Nernst-Planck equation for the diffusion of individual charged species in a porous medium contains thus two main contributions:

- a contribution related to the gradient of activity, $-D_{i,e}c_i\frac{\partial \ln\left(c_i\gamma_i\right)}{\partial x}$,
- and a contribution related to the diffusion potential $+z_iD_{i,e}c_i\frac{\sum_j z_jD_{j,e}c_j\frac{\partial \ln\left(c_j\gamma_j\right)}{\partial x}}{\sum_j z_j^2D_{j,e}c_j}$, which arises from the different mobilities of the diffusing species and the zero electrical current condition.

The contribution related to the gradient of activity can be itself split in two contributions:

- a contribution related to the gradient of concentration $-D_{i,e}\frac{\partial c_i}{\partial x}$, that corresponds to the Fickian diffusion contribution;
- and a contribution related to the gradient of activity coefficient $-D_{i,e}c_i\frac{\partial \ln \gamma_i}{\partial x}$.

If the diffusive transport processes take place in the presence of a spatially homogeneous background electrolyte composition the contribution of the activity coefficient gradient can be omitted and Eq. (11) is simplified to:

$$J_{i,p}^x = -D_{i,e}\frac{\partial c_i}{\partial x} + z_ic_iD_{i,e}\frac{\sum_j z_jD_{j,e}\frac{\partial c_j}{\partial x}}{\sum_j z_j^2D_{j,e}c_j} \tag{12}$$

In addition, if all species have the same diffusion coefficient D_e, Eq. (12) is simplified into:

$$J_{i,p}^x = -D_e\frac{\partial c_i}{\partial x} + z_ic_iD_e\frac{\sum_j z_j\frac{\partial c_j}{\partial x}}{\sum_j z_j^2c_j} \tag{13}$$

Because of the electro-neutrality condition in solution $\sum_j z_j\frac{\partial c_j}{\partial x}$ is equal to zero, and Eq. (13) reduces then to the Fickian diffusion equation:

$$J_{i,p}^x = -D_e\frac{\partial c_i}{\partial x} \tag{14}$$

3 Problem

In the finite difference/volume numerical resolution scheme that is common to most of the reactive transport codes (Steefel et al., 2015), the properties of the media, i.e. porosity, tortuosity,

and local concentrations, are defined at the center for each grid cell and apply to the whole of each grid cell. The flux terms, in contrast, have to be evaluated at the interface between two cells. The activity or concentration gradients between two adjacent cells can be evaluated directly for this purpose. However, Eqs. (11), (12) and (14) contain several terms that must be averaged over two adjacent cells. After discretization, with consideration of activity gradients Eq. (11) becomes:

$$J_{i,p}^{x} = -\overline{D_{i,e}c_i}\frac{\Delta\ln\left(c_i\gamma_i\right)}{\Delta x} + z_i\overline{D_{i,e}c_i}\frac{\sum_j z_j\overline{D_{j,e}c_j}\dfrac{\Delta\ln\left(c_j\gamma_j\right)}{\Delta x}}{\sum_j z_j^2\overline{D_{j,e}c_j}} \tag{15}$$

For the case where activity coefficient gradients are not considered, Eqs. (12) and (14) become, respectively:

$$J_{i,p}^{x} = -\overline{D_{i,e}}\frac{\Delta c_i}{\Delta x} + z_i\overline{D_{i,e}c_i}\frac{\sum_j z_j\overline{D_{j,e}}\dfrac{\Delta c_j}{\Delta x}}{\sum_j z_j^2\overline{D_{j,e}c_j}} \tag{16}$$

$$J_{i,p}^{x} = -\overline{D_{i,e}}\frac{\Delta c_i}{\Delta x} \tag{17}$$

where $\overline{X}$ represent an average value of the parameter X at the interface between two grid cells. Reminding that $\overline{ABC}$, the average of A×B×C, is not equal to $\overline{A}\times\overline{B}\times\overline{C}$, the product of the average values, in general, the discretization method on a grid makes it necessary to define proper averaging methods for the mean values present in Eqs. (15), (16) and (17).

Most reactive transport codes handle only Fickian diffusion (Eq. (17)), but some can handle the Nernst-Planck equation which includes the diffusion potential term (Eqs. (15) and (16); *e.g.* Flotran, Crunchflow, MIN3P, and PHREEQC) (Steefel et al., 2015). Among them, only PHREEQC resolves the dependence of the flux to the activity coefficient gradient (Appelo & Wersin, 2007; Appelo et al., 2010; Appelo, 2017). In the Fickian approximation, it is only necessary to define a proper evaluation of $\overline{D_e}$. Otherwise it is necessary to define the averaging method for $\overline{D_{i,e}c_i}$ and $\overline{D_{i,e}}$. In the following, rigorous averaging methods are derived for all of these terms, and the influence of the averaging methods on the computed diffusive flux is investigated.

4 Mean diffusion transport parameters in two adjacent grid cells

4.1 Fickian approximation and average value of $\overline{D_e}$ at interface

In the case where the Fick's diffusion equation applies, the flux $J_{i,p,1\to2}^{x}$ from grid cell 1 to grid cell 2 can be written:

$$J_{i,p,1\to2}^{x} = -\overline{D_e}\frac{c_{i,2}-c_{i,1}}{\dfrac{\Delta x_2}{2}+\dfrac{\Delta x_1}{2}} \tag{18}$$

where subscripts 1 and 2 indicate that the values are referred to cell 1 and cell 2 respectively. Δx_1 and Δx_2 are the lengths of grid cells 1 and 2 respectively. It is also possible to define $J^x_{i,p,1\to\text{int}}$ and $J^x_{i,p,\text{int}\to 2}$, the flux from the center of cell 1 to the interface and from the interface to the center of cell 2, where the subscript "int" indicates that the values are referred to the interface between the two cells. The properties within each cell are homogeneous, and it follows:

$$J^x_{i,p,1\to\text{int}} = -D_{e,1}\frac{c_{i,\text{int}} - c_{i,1}}{\frac{\Delta x_1}{2}} \tag{19}$$

$$J^x_{i,p,\text{int}\to 2} = -D_{e,2}\frac{c_{i,2} - c_{i,\text{int}}}{\frac{\Delta x_2}{2}} \tag{20}$$

Under stationary conditions:

$$J^x_{i,p,1\to\text{int}} = J^x_{i,p,\text{int}\to 2} = J^x_{i,p,1\to 2} \tag{21}$$

and thus:

$$c_{i,\text{int}} = \frac{D_{e,2}c_{i,2}\Delta x_1 + D_{e,1}c_{i,1}\Delta x_2}{D_{e,2}\Delta x_1 + D_{e,1}\Delta x_2} \tag{22}$$

Eq. (22) can be reinserted in Eq. (21):

$$\overline{D_e} = \frac{D_{e,2}D_{e,1}\left(\Delta x_2 + \Delta x_1\right)}{D_{e,2}\Delta x_1 + D_{e,1}\Delta x_2} \tag{23}$$

At steady state, the value of the effective diffusion coefficient at the interface $\overline{D_{i,e}}$ is thus the weighted harmonic mean of $D_{i,e,2}$ and $D_{i,e,1}$.

4.2 Average concentration to be used in the Nernst-Planck equation at interface

Gimmi and Alt-Epping (2018) explored this problem in the specific case of a Donnan membrane system in which a reservoir of electro-neutral solution (subscript 1) was considered to be at equilibrium with another reservoir (subscript 2) that contained fixed charges. The solution in reservoir 2 was not electroneutral, and its charge compensated the fixed charges. The fixed charges were simulated using immobile species ($D_e = 0$), and the system was modeled with the Nernst-Planck equation. The system was considered to be at equilibrium when the diffusion fluxes were equal to zero for each of the species. Because of the presence of the fixed charges in the reservoir 2, solute species concentrations were not equal in reservoirs 1 and 2 at equilibrium (zero flux condition). In these conditions, they were able to show analytically and numerically that the average concentration at the interface, $c_{i,int}$, should be calculated for all mobile species according to:

$$c_{i,int} = \frac{c_{i,2} - c_{i,1}}{\ln c_{i,2} - \ln c_{i,1}} \tag{24}$$

184 It is possible to generalize this result to any diffusion problem in transient non-equilibrium
185 conditions. The activity gradient terms in the Nernst-Planck equation can be expanded into:

$$D_{i,e}c_i\frac{\partial \ln\left(c_i\gamma_i\right)}{\partial x} = D_{i,e}c_i\frac{\partial \ln c_i}{\partial x} + D_{i,e}c_i\frac{\partial \ln \gamma_i}{\partial x} \tag{25}$$

186 and the concentration gradient term must respect the following mathematical equality:

$$D_{i,e}c_i\frac{\partial \ln c_i}{\partial x} = D_{i,e}\frac{\partial c_i}{\partial x} \tag{26}$$

187 It follows after discretization on a grid:

$$\overline{D_{i,e}c_i}\frac{\Delta \ln c_i}{\Delta x} = \overline{D_{i,e}}\frac{\Delta c_i}{\Delta x} \tag{27}$$

188 and thus, between two cells 1 and 2:

$$\overline{D_{i,e}c_i} = \overline{D_{i,e}}\frac{c_{i,2}-c_{i,1}}{\ln c_{i,2} - \ln c_{i,1}} \tag{28}$$

189 In a medium with spatially homogeneous properties (constant $D_{i,e}$ value), or generally when the
190 average $\overline{D_e}$ is independent of the concentrations c_i (as is the case for Eq. (23) as long as the local
191 $D_{i,e}$ are independent of the pore water chemistry), Eq. (28) becomes:

$$\overline{c_i} = \frac{c_{i,2}-c_{i,1}}{\ln c_{i,2} - \ln c_{i,1}} \tag{29}$$

192 Eq. (29) is identical to Eq. (24), but it was obtained for a more general case, *i.e.* without
193 requiring equilibrium or steady-state conditions, and without the presence of immobile solute
194 species. One must note that the terms related to the activity coefficient gradient cancel in Eq.
195 (25), thus the condition of the absence of activity coefficient gradients is not necessary to apply
196 in Eq. (28) or (29).

197 This result shows that the simplifications made from Eq. (11) to (12) with the equality
198 $\frac{\partial \ln y}{\partial x} = \frac{1}{y}\frac{\partial y}{\partial x}$ might result in reduced accuracy of the results obtained after spatial discretization
199 on a grid. In spatially heterogeneous media, and without any assumptions about equilibrium or
200 steady-state conditions, Eq. (28) can be combined directly with Eq. (15) to yield:

$$J_{i,p}^{x} = -\overline{D_{i,e}}\left(\frac{\Delta c_i}{\Delta x} + \frac{\Delta c_i}{\Delta \ln c_i}\frac{\Delta \ln \gamma_i}{\Delta x}\right) + z_i\overline{D_{i,e}}\frac{\Delta c_i}{\Delta \ln c_i}\frac{\sum_j z_j\overline{D_{j,e}}\left(\frac{\Delta c_j}{\Delta x} + \frac{\Delta c_j}{\Delta \ln c_j}\frac{\Delta \ln \gamma_j}{\Delta x}\right)}{\sum_j z_j^2\overline{D_{j,e}}\frac{\Delta c_j}{\Delta \ln c_j}} \tag{30}$$

201

202 Neglecting the activity coefficient gradients:

$$J_{i,p}^{x} = -\overline{D_{i,e}}\frac{\Delta c_i}{\Delta x} + z_i \overline{D_{i,e}}\frac{\Delta c_i}{\Delta \ln c_i}\frac{\sum_j z_j \overline{D_{j,e}}\frac{\Delta c_j}{\Delta x}}{\sum_j z_j^2 \overline{D_{j,e}}\frac{\Delta c_j}{\Delta \ln c_j}} \quad (31)$$

Eq. (31) leaves $\overline{D_{i,e}}$ as the only average parameter that must be evaluated at the interface between two grid cells in a spatially heterogeneous system. In any case, the value of $\overline{D_{i,e}}$ can be obtained with Eq. (23), as the $\overline{D_{i,e}}$ values that enter the Nernst-Planck equation have to represent the species diffusion coefficients without considering any coupling between different ions, *i.e.*, just for Fickian transport. Accordingly, Eq. (23) can thus be combined to Eq. (31) to give the general discretized form of the Nernst-Planck equation in a heterogeneous system.

5 Evaluation of alternative averaging methods on the computation of diffusive fluxes

Reactive transport codes use different types of averaging methods to evaluate the diffusion parameters at interfaces between cells (Tournassat & Steefel, 2019a), and the influence of averaging schemes that are different from the correct one, which is given by Eq. (31) combined with Eq. (23), should then be evaluated. Two simple model systems were set-up to illustrate these differences.

The first system was made by two reservoirs separated by a membrane. Na^+ and Cl^- concentrations were set to 0.1 mol·L^{-1} in the left reservoir and in the membrane, while the right reservoir contained a solution of 1 mol·L^{-1} Cl^-, 2 mol·L^{-1} Na^+, and 1 mol·L^{-1} of a large monovalent anionic molecule for which the membrane was impermeable. To this end, a tortuosity factor of zero was specifically assigned to this species in the membrane. Consequently, all species were able to diffuse through the membrane except the large anionic molecule. The tortuosity factor of the reservoirs and membrane were set otherwise to 1 for all species. Self-diffusion coefficients (D_0) were set to 1.3 10^{-9} m^2·s^{-1}, 2.1 10^{-9} m^2·s^{-1}, and 10^{-9} m^2·s^{-1} for Na^+, Cl^- and the large anionic species. The length of the two reservoirs (porosity of 1) was set to 5 mm and the thickness of the membrane (porosity of 0.1) was set to 200 µm (Figure 1). Each of the reservoir domains was discretized into 25 grid cells. The second system differed from the first one by the absence of the membrane between the two reservoirs, by the size of the grid cells in the left reservoir (100 µm for a total length of 2.5 mm) and by the presence of different tortuosity factors for the different species in the two reservoirs: 0.5 for all species in the left reservoir, and 1, 0.7 and 0.2 for Na^+, Cl^- and the large anionic species respectively in the right reservoir (Figure 2). The charge of the large anionic molecule was also set to -2 and its concentration was decreased to 0.5 mol·L^{-1}. Three different averaging methods were tested: the reference method given by Eq. (31) combined with Eq. (23), and two alternative methods described in Table 1. The alternative method 1 lumped together the effective diffusion coefficient and the concentration before harmonic averaging at the interface, while the alternative method 2 computed the harmonic average of $D_{i,e}$ and multiplied it with the weighted arithmetic average concentration at the interface. The diffusion calculations were run using the code 3Diff with an explicit, forward in time and central in space, numerical resolution scheme. This code and its resolution scheme have been benchmarked successfully with CrunchClay and PHREEQC using the arithmetic average method (alternative method 2) (Tournassat & Steefel, 2019a).

The system 1 is representative of a semi-permeable membrane system for which a Donnan equilibrium is expected after equilibration. Indeed, the reference model predicted the correct concentrations in the right reservoir corresponding to the Donnan equilibrium (Figure 1, left), a result that was consistent with previous findings of Gimmi and Alt-Epping (2018), who showed the importance of using a logarithmic average for the computation of the concentration at the interface between two cells when solving the Nernst-Planck equation in the presence of immobile species. The alternative method 2 also made it possible to predict the correct concentration, but only far from the membrane-reservoir interfaces. Next to this interface, charge balance problems occurred, and electroneutrality was not achieved on both sides of the membrane. This problem illustrates the need to compute correctly the average concentrations in the interfacial terms of the Nernst-Planck equation. The alternative method 1 resulted in large deviations from electroneutrality, which ultimately led to large concentration oscillations in the numerical solution of the transport equation (Figure 1, right). In system 2, which is very heterogeneous, the reference and the alternative method 2 led to similar results, while the alternative method 1 resulted in large concentration oscillations after ~300 s of simulated time (Figure 2). The alternative method 2 (arithmetic averaging) is the method commonly used in reactive transport modeling codes. Our simple intercomparison exercise pointed out the adequacy of the arithmetic averaging method for problems, in which membrane behavior and large electrolyte concentration gradients are not present.

Table 1. Equations for the evaluation of diffusive flux as a function of averaging methods for interfacial properties.

	Flux equation	Averaged terms at the interface
Reference method	$J^x_{i,p} = -\overline{D_{i,e}}\frac{\Delta c_i}{\Delta x} + z_i \overline{D_{i,e}} \frac{\Delta c_i}{\Delta \ln c_i} \frac{\sum_j z_j \overline{D_{j,e}} \frac{\Delta c_j}{\Delta x}}{\sum_j z_j^2 \overline{D_{j,e}} \frac{\Delta c_j}{\Delta \ln c_j}}$	$\overline{c_i} = \frac{\ln c_{i,1} - \ln c_{i,2}}{c_{i,1} - c_{i,2}}$ $\overline{D_{i,e}} = \frac{D_{i,e,2} D_{i,e,1} (\Delta x_2 + \Delta x_1)}{D_{i,e,2}\Delta x_1 + D_{i,e,1}\Delta x_2}$
Alternative method 1	$J^x_{i,p} = -\overline{D_{i,e}}\frac{\Delta c_i}{\Delta x} + z_i \overline{D_{i,e} c_i} \frac{\sum_j z_j \overline{D_{j,e}} \frac{\Delta c_j}{\Delta x}}{\sum_j z_j^2 \overline{D_{j,e} c_j}}$	$\overline{D_{i,e} c_i} = \frac{D_{e,2} c_{i,2} \Delta x_1 D_{e,1} c_{i,1} \Delta x_2}{D_{e,2} c_{i,2} \Delta x_1 + D_{e,1} c_{i,1} \Delta x_2}$ $\overline{D_{i,e}} = \frac{D_{i,e,2} D_{i,e,1} (\Delta x_2 + \Delta x_1)}{D_{i,e,2}\Delta x_1 + D_{i,e,1}\Delta x_2}$
Alternative method 2	$J^x_{i,p} = -\overline{D_{i,e}}\frac{\Delta c_i}{\Delta x} + z_i \overline{D_{i,e}}\,\overline{c_i} \frac{\sum_j z_j \overline{D_{j,e}} \frac{\Delta c_j}{\Delta x}}{\sum_j z_j^2 \overline{D_{j,e}}\,\overline{c_j}}$	$\overline{c_i} = \frac{c_{i,1}\Delta x_1 + c_{i,2}\Delta x_2}{\Delta x_1 + \Delta x_2}$ $\overline{D_{i,e}} = \frac{D_{i,e,2} D_{i,e,1} (\Delta x_2 + \Delta x_1)}{D_{i,e,2}\Delta x_1 + D_{i,e,1}\Delta x_2}$

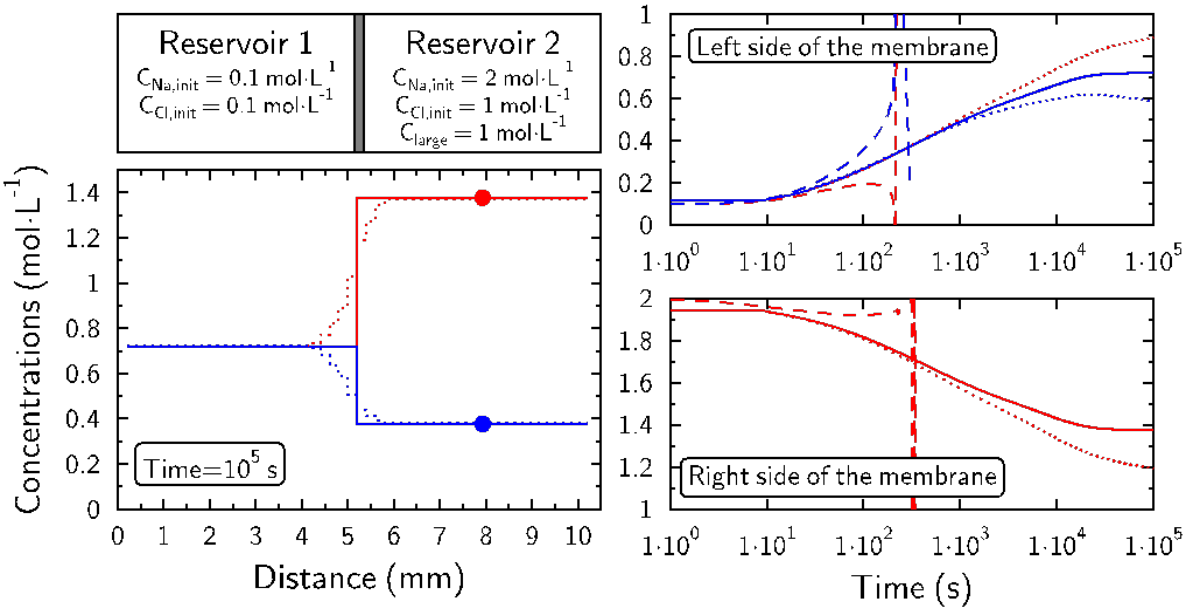

Figure 1. Top left: system 1 under investigation. The gray area represents the membrane (thickness=200 µm) that separates the two reservoirs (length=5 mm each), and which is impermeable to the large anionic molecules. Initial Na^+, Cl^- and large anionic molecule concentrations are indicated for each reservoir. Bottom left: Na^+ (red) and Cl^- (blue) concentration profiles obtained after 10^5 s of diffusion. The two circles at x=8 mm indicate the concentration expected in reservoir 2 according to Donnan equilibrium. Plain line: reference model. Dotted line: alternative model 2. Right: Na^+ (red) and Cl^- (blue) concentration on the left (top) and right (bottom) side of the membrane as a function of time and predicted with the different models. Plain line: reference model. Dashed line: alternative model 1. Dotted line: alternative model 2. Note that the calculation becomes unstable with the alternative model 1 after ~300 s of simulated time because of charge balance issues, and that electroneutrality was not achieved next to the membrane with the alternative model 2.

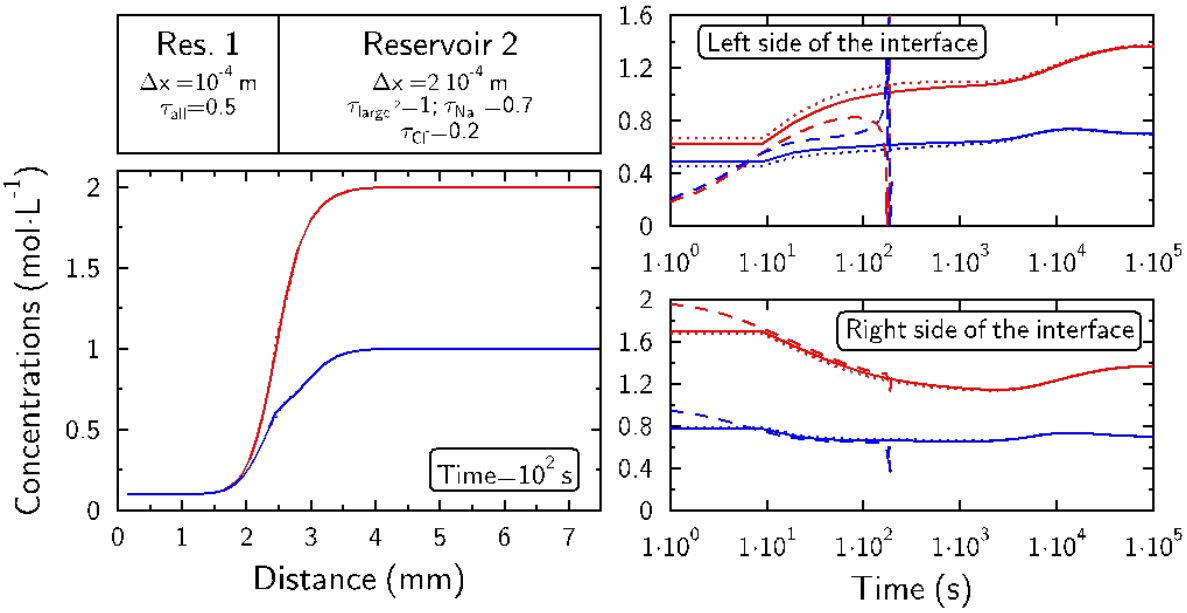

Figure 2. Top left figure: heterogeneous system 2 under investigation. Initial Na^+, Cl^- are the same as in system 1. The large anionic molecule concentration was two times lower, while its charge was set to -2 instead of -1. Grid cell discretization and tortuosity factors are indicated in the figure. Bottom left figure: Na^+ (red) and Cl^- (blue) concentration profiles obtained after 100 s of diffusion. Plain line: reference model. Dotted line: alternative model 2. Right figure: Na^+ (red) and Cl^- (blue) concentration on the left (top) and right (bottom) side of the interface between the two reservoirs as a function of time and predicted with the different models. Plain line: reference model. Dashed line: alternative model 1. Dotted line: alternative model 2. Note that the calculation becomes unstable with the alternative model 1 after ~300 s of simulated time because of charge balance issues.

6 Conclusions

In the present study, the proper numerical method was defined to average the concentrations of dissolved species and the porous media properties at the interface between two grid cells in order to solve the Nernst-Planck equation with a finite difference/volume method. The computation of the weighted arithmetic average (alternative method 2) has been historically the averaging procedure that is used in most reactive transport codes that can solve the Nernst Planck equations. Our results emphasize the necessity to change this averaging method to one based on a logarithmic-differential average, *i.e.* the reference method demonstrated in the present study, and proposed previously by Gimmi and Alt-Epping (2018). The resulting improvement in the numerical stability and in the accuracy of concentration prediction is especially necessary to model semi-permeable membrane properties such as those used in water treatment processes.

Acknowledgments

This work was supported by the Office of Science, Office of Basic Energy Sciences, of the U.S. Department of Energy (BES-DOE) under Contract No. DE-AC02-05CH11231, by the Agence Nationale de la Recherche (ANR) under Contract No. ANR-18-CE05-0035-01, by the European

Project EURAD DONUT, and by the Swiss National Cooperative for the Disposal of Radioactive Waste (Nagra).

References

Anna, P. de, Le Borgne, T., Dentz, M., Bolster, D., Davy, P., 2011. Anomalous kinetics in diffusion limited reactions linked to non-Gaussian concentration probability distribution function. *The Journal of chemical physics* 135, 174104.

Anna, P. de, Jimenez-Martinez, J., Tabuteau, H., Turuban, R., Le Borgne, T., Derrien, M., Méheust, Y., 2013. Mixing and reaction kinetics in porous media: an experimental pore scale quantification. *Environmental science & technology* 48, 508–516.

Appelo, C.A.J., 2017. Solute transport solved with the Nernst-Planck equation for concrete pores with "free" water and a double layer. *Cement and Concrete Research* 101, 102–113.

Appelo, C.A.J., Van Loon, L.R., Wersin, P., 2010. Multicomponent diffusion of a suite of tracers (HTO, Cl, Br, I, Na, Sr, Cs) in a single sample of Opalinus clay. *Geochimica et Cosmochimica Acta* 74, 1201–1219.

Appelo, C.A.J., Vinsot, A., Mettler, S., Wechner, S., 2008. Obtaining the porewater composition of a clay rock by modeling the in- and out-diffusion of anions and cations from an in-situ experiment. *Journal of Contaminant Hydrology* 101, 67–76.

Appelo, C.A.J., Wersin, P., 2007. Multicomponent diffusion modeling in clay systems with application to the diffusion of tritium, iodide, and sodium in Opalinus clay. *Environmental Science & Technology* 41, 5002–5007.

La Bolle, E.M., Fogg, G.E., 2001. Role of molecular diffusion in contaminant migration and recovery in an alluvial aquifer system. *Transport in Porous Media* 42, 155–179.

La Bolle, E.M., Fogg, G.E., Eweis, J.B., Gravner, J., Leaist, D.G., 2008. Isotopic fractionation by diffusion in groundwater. *Water Resources Research* 44.

Bone, S.E., Cahill, M.R., Jones, M.E., Fendorf, S., Davis, J., Williams, K.H., Bargar, J.R., 2017. Oxidative uranium release from anoxic sediments under diffusion-limited conditions. *Environmental Science & Technology* 51, 11039–11047.

Le Borgne, T., Dentz, M., Davy, P., Bolster, D., Carrera, J., De Dreuzy, J.-R., Bour, O., 2011. Persistence of incomplete mixing: A key to anomalous transport. *Physical Review E* 84, 015301.

Le Borgne, T., Dentz, M., Villermaux, E., 2013. Stretching, coalescence, and mixing in porous media. *Physical review letters* 110, 204501.

Boudreau, B.P., Meysman, F.J., Middelburg, J.J., 2004. Multicomponent ionic diffusion in porewaters: Coulombic effects revisited. *Earth and Planetary Science Letters* 222, 653–666.

Bourg, I.C., Richter, F.M., Christensen, J.N., Sposito, G., 2010. Isotopic mass dependence of metal cation diffusion coefficients in liquid water. *Geochimica et Cosmochimica Acta* 74, 2249–2256.

Bourg, I.C., Sposito, G., 2007. Molecular dynamics simulations of kinetic isotope fractionation during the diffusion of ionic species in liquid water. *Geochimica et Cosmochimica Acta* 71, 5583–5589.

Bourg, I.C., Tournassat, C., 2015. Chapter 6 - Self-diffusion of water and ions in clay barriers. In: Tournassat, C., Steefel, C.I., Bourg, I.C., Bergaya, F. (Eds.), *Natural and Engineered Clay Barriers*, *Developments in Clay Science*. Elsevier, pp. 71–100.

Chapman, S.W., Parker, B.L., 2005. Plume persistence due to aquitard back diffusion following dense nonaqueous phase liquid source removal or isolation. *Water Resources Research* 41.

Chiogna, G., Cirpka, O.A., Grathwohl, P., Rolle, M., 2011. Relevance of local compound-specific transverse dispersion for conservative and reactive mixing in heterogeneous porous media. *Water Resources Research* 47.

Alt-Epping, P., Gimmi, T., Wersin, P., Jenni, A., 2018. Incorporating electrical double layers into reactive-transport simulations of processes in clays by using the Nernst-Planck equation: A benchmark revisited. *Applied Geochemistry* 89, 1–10.

Alt-Epping, P., Tournassat, C., Rasouli, P., Steefel, C.I., Mayer, K.U., Jenni, A., Mäder, U., Sengor, S.S., Fernandez, R., 2015. Benchmark reactive transport simulations of a column experiment in compacted bentonite with multispecies diffusion and explicit treatment of electrostatic effects. *Computational Geosciences* 19, 535–550.

Felmy, A.R., Weare, J.H., 1991a. Calculation of multicomponent ionic diffusion from zero to high concentration: I. The system Na-K-Ca-Mg-Cl-SO4-H2O at 25 C. *Geochimica et Cosmochimica Acta* 55, 113–131.

Felmy, A.R., Weare, J.H., 1991b. Calculation of multicomponent ionic diffusion from zero to high concentration: II. Inclusion of associated ion species. *Geochimica et Cosmochimica Acta* 55, 133–144.

Giambalvo, E.R., Steefel, C.I., Fisher, A.T., Rosenberg, N.D., Wheat, C.G., 2002. Effect of fluid-sediment reaction on hydrothermal fluxes of major elements, eastern flank of the Juan de Fuca Ridge. *Geochimica et Cosmochimica Acta* 66, 1739–1757.

Gimmi, T., Alt-Epping, P., 2018. Simulating Donnan equilibria based on the Nernst-Planck equation. *Geochimica et Cosmochimica Acta* 232, 1–13.

Glaus, M., Aertsens, M., Appelo, C., Kupcik, T., Maes, N., Van Laer, L., Van Loon, L., 2015. Cation diffusion in the electrical double layer enhances the mass transfer rates for Sr2+, Co2+ and Zn2+ in compacted illite. *Geochimica et Cosmochimica Acta* 165, 376–388.

Glaus, M.A., Birgersson, M., Karnland, O., Van Loon, L.R., 2013. Seeming steady-state uphill diffusion of $^{22}Na^{+}$ in compacted montmorillonite. *Environmental Science & Technology* 47, 11522–11527.

Gouze, P., Melean, Y., Le Borgne, T., Dentz, M., Carrera, J., 2008. Non-Fickian dispersion in porous media explained by heterogeneous microscale matrix diffusion. *Water Resources Research* 44.

Gvirtzman, H., Gorelick, S., 1991. Dispersion and advection in unsaturated porous media enhanced by anion exclusion. *Nature* 352, 793.

Hadley, P.W., Newell, C., 2014. The new potential for understanding groundwater contaminant transport. *Groundwater* 52, 174–186.

Haghighi, E., Shahraeeni, E., Lehmann, P., Or, D., 2013. Evaporation rates across a convective air boundary layer are dominated by diffusion. *Water Resources Research* 49, 1602–1610.

Lasaga, A.C., 1979. The treatment of multi-component diffusion and ion pairs in diagenetic fluxes. *American Journal of Science* 279, 324–346.

Liu, C., Shang, J., Zachara, J.M., 2011. Multispecies diffusion models: A study of uranyl species diffusion. *Water Resources Research* 47.

Liu, C., Zachara, J.M., Yantasee, W., Majors, P.D., McKinley, J.P., 2006. Microscopic reactive diffusion of uranium in the contaminated sediments at Hanford, United States. *Water Resources Research* 42.

Marcus, A.K., Torres, C.I., Rittmann, B.E., 2010. Evaluating the impacts of migration in the biofilm anode using the model PCBIOFILM. *Electrochimica Acta* 55, 6964–6972.

Muniruzzaman, M., Haberer, C.M., Grathwohl, P., Rolle, M., 2014. Multicomponent ionic dispersion during transport of electrolytes in heterogeneous porous media: Experiments and model-based interpretation. *Geochimica et Cosmochimica Acta* 141, 656–669.

Muniruzzaman, M., Rolle, M., 2015. Impact of multicomponent ionic transport on pH fronts propagation in saturated porous media. *Water Resources Research* 51, 6739–6755.

Muniruzzaman, M., Rolle, M., 2016. Modeling multicomponent ionic transport in groundwater with IPhreeqc coupling: Electrostatic interactions and geochemical reactions in homogeneous and heterogeneous domains. *Advances in water resources* 98, 1–15.

Muniruzzaman, M., Rolle, M., 2017. Experimental investigation of the impact of compound-specific dispersion and electrostatic interactions on transient transport and solute breakthrough. *Water Resources Research* 53, 1189–1209.

Peeters, F., Beyerle, U., Aeschbach-Hertig, W., Holocher, J., Brennwald, M.S., Kipfer, R., 2002. Improving noble gas based paleoclimate reconstruction and groundwater dating using 20Ne/22Ne ratios. *Geochimica et Cosmochimica Acta* 67, 587–600.

Rasouli, P., Steefel, C.I., Mayer, K.U., Rolle, M., 2015. Benchmarks for multicomponent diffusion and electrochemical migration. *Computational Geosciences* 1–11.

Robinet, J.-C., Sardini, P., Coelho, D., Parneix, J.-C., Prêt, D., Sammartino, S., Boller, E., Altmann, S., 2012. Effects of mineral distribution at mesoscopic scale on solute diffusion in a clay-rich rock: Example of the Callovo-Oxfordian mudstone (Bure, France). *Water Resources Research* 48, W05554.

Rolle, M., Chiogna, G., Bauer, R., Griebler, C., Grathwohl, P., 2010. Isotopic fractionation by transverse dispersion: Flow-through microcosms and reactive transport modeling study. *Environmental science & technology* 44, 6167–6173.

Rolle, M., Sprocati, R., Masi, M., Jin, B., Muniruzzaman, M., 2018. Nernst-Planck-based description of transport, coulombic interactions, and geochemical reactions in porous media: Modeling approach and benchmark experiments. *Water Resources Research* 54, 3176–3195.

Shackelford, C.D., 1991. Laboratory diffusion testing for waste disposal – A review. *Journal of Contaminant Hydrology* 7, 177–217.

Steefel, C.I., Appelo, C.A.J., Arora, B., Jacques, D., Kalbacher, T., Kolditz, O., Lagneau, V., Lichtner, P.C., Mayer, K.U., Meeussen, J.C.L., Molins, S., Moulton, D., Shao, H., Šimunek, J., Spycher, N., Yabusaki, S.B., Yeh, G.T., 2015. Reactive transport codes for subsurface environmental simulation. *Computational Geosciences* 19, 445–478.

Steefel, C.I., Maher, K., 2009. Fluid-rock interaction: A reactive transport approach. *Reviews in Mineralogy and Geochemistry* 70, 485–532.

Tinnacher, R.M., Holmboe, M., Tournassat, C., Bourg, I.C., Davis, J.A., 2016. Ion adsorption and diffusion in smectite: molecular, pore, and continuum scale views. *Geochimica et Cosmochimica Acta* 177, 130–149.

Tokunaga, T.K., Shen, W., Wan, J., Kim, Y., Cihan, A., Zhang, Y., Finsterle, S., 2017. Water Saturation Relations and Their Diffusion-Limited Equilibration in Gas Shale:

438 Implications for Gas Flow in Unconventional Reservoirs. *Water Resources Research* 53,
439 9757–9770.
440 Tournassat, C., Steefel, C.I., 2015. Ionic transport in nano-porous clays with consideration of
441 electrostatic effects. *Reviews in Mineralogy and Geochemistry* 80, 287–330.
442 Tournassat, C., Steefel, C.I., 2019a. Modeling diffusion processes in the presence of a diffuse
443 layer at charged mineral surfaces. A benchmark exercise. *Computational Geosciences*.
444 Tournassat, C., Steefel, C.I., 2019b. Reactive transport modeling of coupled processes in
445 nanoporous media. *Reviews in Mineralogy and Geochemistry* 85, 75–110.
446 Ben-Yaakov, S., 1972. Diffusion of sea water ions–I. Diffusion of sea water into a dilute
447 solution. *Geochimica et Cosmochimica Acta* 36, 1395–1406.
448 Zachara, J., Brantley, S., Chorover, J., Ewing, R., Kerisit, S., Liu, C., Perfect, E., Rother, G.,
449 Stack, A.G., 2016. Internal domains of natural porous media revealed: critical locations
450 for transport, storage, and chemical reaction. *Environmental Science & Technology* 50,
451 2811–2829.
452